NISTIR 7902

Fatigue Flaw NDE Reference Standard Development Phase I—Feasibility Study

Mark D. Richards
J. David McColskey
Timothy S. Weeks

http://dx.doi.org/10.6028/NIST.IR.7902

National Institute of Standards and Technology
U.S. Department of Commerce

NISTIR 7902

Fatigue Flaw NDE Reference Standard Development Phase I—Feasibility Study

Mark D. Richards
J. David McColskey
Timothy S. Weeks
Applied Chemicals and Materials Division
Material Measurement Laboratory

http://dx.doi.org/10.6028/NIST.IR.7902

November 2012

U.S. Department of Commerce
Rebecca Blank, Acting Secretary

National Institute of Standards and Technology
Patrick D. Gallagher, Under Secretary of Commerce for Standards and Technology and Director

Abstract

A feasibility study was performed to evaluate a novel method of accurately fatigue-cracking steel plates to generate proposed fatigue-crack reference standards. Fatigue cracks were introduced into low-carbon steel reference plates and the actual size of the fatigue cracks were accurately predicted by the fatigue-crack introduction technique. Flaw sizing of the fatigue cracks in the plates was conducted by industrial collaborators through use of various nondestructive evaluation (NDE) techniques. As part of the feasibility study, a limited round robin analysis was conducted that included NDE sensor manufacturers and users, that demonstrated the fatigue cracks in the reference plates could be located and sized. The round robin demonstrated significant scatter in the NDE data, and the crack depth and surface breaking length values ($a \times 2c$) were both over-and under-predicted as compared to the actual values of the reference plates. The NDE community acknowledges a genuine need for a fatigue crack reference standard by which NDE sensors and technologies can be calibrated and verified for the accurate sizing of fatigue flaws in structural components.

Keywords

Artifact, fatigue crack, flaw sizing, NDE, non-destructive evaluation, phased array ultrasonic, reference standard.

Table of Contents

1. Introduction

Nondestructive evaluation (NDE)[1] techniques are widely used to detect flaws in critical structures in chemical processing facilities, nuclear reactors, oil and gas pipelines, bridges and other infrastructure. If these flaws are undetected, they can compromise the integrity of the structure and potentially lead to catastrophic failure, extensive property damage, injury, and in many cases, loss of human life. More recently, structural designers have adopted a "damage-tolerant" design with use of engineering critical assessment (ECA). In this paradigm, components having known defects can continue in service as long as models predict that the defects will not grow to a critical, failure-producing size. As a result, the simple detection of defects is insufficient; accurate flaw sizing is critical for predicting the remaining service life of a given structure [1], and determining structural reliability and prediction of structural lifetime [2].

Reference standards[2] are used as calibration tools for NDE systems and are critical both to establish a general level of consistency in measurements and to help interpret and quantify the information contained in the received signal. They ensure that the equipment and the setup provide similar results from one day to the next and that similar results are produced by different systems and different inspectors. They can also help the inspector estimate the size of flaws. For example, ultrasonic testing (UT), the most common of the inspection techniques described here, employs high-frequency (typically from 2×10^5 Hz to a maximum of 10^7 Hz) sound energy to detect flaws and make measurements. In a UT pulse-echo type setup, signal strength depends on both the size of the flaw and the distance between the flaw and the transducer. The inspector can use a reference standard to produce a signal from an artificially-induced flaw of known size and distance from the transducer. By comparing the signal from the reference standard to that received from the actual flaw, the inspector can detect the flaw and gain some insight about its size. However, precise flaw sizing is not possible with this technique.

An example of a current reference standard is a block described by the International Institute of Welding. This block is machined from a material that is acoustically similar to the material to be tested. The block has several "defects" that are machined into it for calibration purposes, including machined right circular cylindrical holes, notches and surfaces. While these "defects" are precisely machined, they are not representative of true flaws in a structure and do not provide a calibration standard for NDT equipment sufficient for accurate flaw sizing. In most cases, artificially induced defects more efficiently reflect sound energy (due to their flatter, smoother, machined surfaces) and produce indications that are larger than those that a similar sized actual flaw (fatigue crack, weld defect, wall thinning due to corrosion, etc.) would produce. Accurate characterization of fatigue cracks is difficult, because the contact of surface asperities during crack closure makes the crack nearly transparent to the ultrasonic wave [2]. A significant challenge in quantifying the performance of NDE techniques for their accuracy and reliability for probability of detection and flaw sizing is the development of reference artifacts that contain representative cracks or discontinuities [3]. For this reason, the industry requires reference standards that contain representative, accurately characterized "cracks" to enable methods of accurately sizing of actual flaws in the field**.**

Despite the fact that calibration of NDE instrumentation has been noted as a serious challenge for inspectors, there are no "true-crack" reference artifacts available for instrument calibration that are certified or traceable to standards of known crack dimensions. Such artifacts must be representative of the material to be inspected and precisely characterized with regards to crack size (width, depth and shape). Researchers [4-6] have demonstrated the resulting considerable improvement in flaw-sizing accuracy when a natural flaw was used as a reference standard. However, a reliable method of production of more realistic defects has not been available, and the development of a fatigue crack reference standard has been considered cost prohibitive. Based on techniques developed for growing well-characterized fatigue cracks in machined test specimens

[1] NDE includes, but is not limited to: ultrasonic methods [ultrasonic testing (UT), electromagnetic acoustic transducer (EMAT), phased array ultrasound, and long-range guided wave (LRGW)]; electromagnetic methods [eddy current (EC) and magnetic flux leakage (MFL)]; radiographic methods; thermographic methods; and dynamic methods (resonant frequency and attenuation testing).

[2] The leading standards organizations in this area include the International Standards Organization (ISO), the American Welding Society (AWS) and the American Society for Testing and Materials, International (ASTM). The responsible ISO committee is TC135/SC3, "Ultrasonic Testing"; and the primary standard relative to the proposed SRM is ISO 12715, "Nondestructive testing - Ultrasonic inspection - Reference blocks and test procedures for the characterization of contact search unit beam profiles." AWS provides a related reference block called the IIW (International Institute of Welding) block, and ASTM provides several recommended standards useful in the calibrations of NDT equipment including ASTM E164, E127, E428, E2491, and E797.

[7], the development of standard reference materials (SRMs) containing real cracks can be manufactured at a reasonable cost; and their use will enable more accurate, cost-effective sizing of flaws in pipelines, structural components such as bridges, nuclear power plants and pressure vessels.

2. Methods

2.1 Materials

Two materials were selected and procured for the present standard reference material (SRM) development program. The first material is an API-5L (American Petroleum Institute) X80 linepipe steel [551 MPa (80 ksi) nominal yield strength] that was received in 1.067 m (42 in) outer diameter and 14.5 mm wall thickness condition. Strips of base metal were sectioned from the pipe and made into 254 mm (10 in.) × 254 mm (10 in.) square specimens. The second material is an ASTM A709 grade that has a nominal chemical composition of 0.20 % C, 1.09 % Mn, 0.18 % Ni and 0.52 % Cr by mass with V microalloying additions. The A709 grade was received in two geometries; both were flat plate with a nominal thickness of 25.4 mm, widths of 101.6 mm and 152.2 mm and lengths of 305 mm. The A709 material was supplied with a nominal yield strength of 384 MPa and tensile strength of 562 MPa. Room temperature tensile engineering stress versus strain data for the A709 material are shown in Figure 1.

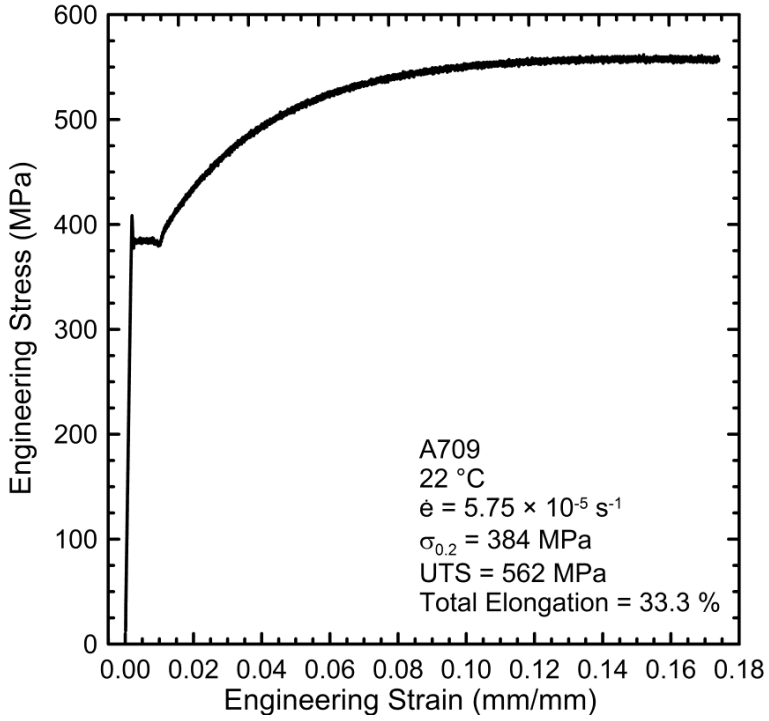

Figure 1 – Tensile engineering stress versus engineering strain data for A709 alloy tested at room temperature at a constant engineering strain rate of $\dot{e} = 5.75 \times 10^{-5}\ s^{-1}$.

2.2 Notching

Fatigue crack starter notches were introduced into the surface of the pipe and plate specimens by use of a sinker type electrical discharge machining (EDM) process. A starter notch is a manufactured stress concentration artifact through which the higher stress intensity generated at the periphery of the starter notch allows for the initiation of fatigue cracks at low applied force levels and allows for the guidance of fatigue crack shape. In the sinker EDM process, an electrode was fabricated and was plunged into the work piece; the resultant arc ablated the work piece material, and a void was formed in the shape of the electrode.

EDM starter notches were machined at the centers of six flat plates, three each from the 4 in. and 6 in. widths. Figure 2 shows the EDM electrode geometry for the 1.4 mm × 23.2 mm (a × 2c) notch geometry used for the 25.4 mm thick flat plate

specimens. The electrode was composed of three parts, two pieces that had a square profile, between which is the smooth arc profile electrode from which the starter notch derives its shape. The two square electrodes were included to provide a sufficient slot for instrumentation that was used for the fatigue-cracking step. This electrode arrangement allowed for the notch to be machined in one step using electrodes 0.20 mm (0.008 in) thick. The notches were cut to a depth of 1.4 mm from the surface and produced a surface-breaking length (2c) of 23.2 mm.

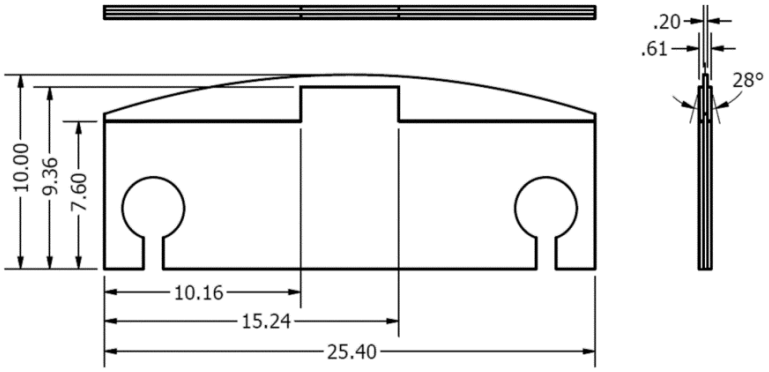

Figure 2 – EDM electrode geometry for the 1.4 mm x 21.2 mm notch geometry for the 4 in. and 6 in. wide, flat plate specimens (units in mm).

EDM starter notches were machined at the center of one pipe segment, while three more segments are awaiting notching, pending analysis by a collaborating NDE analysis company. The electrode geometry for the pipeline is illustrated in Figure 3. Two electrode thicknesses were used for the pipe EDM starter notches, 0.41 mm (0.016 in) thick to a notch depth of 1.55 mm and 0.05 mm (0.002 in) thick to a notch depth of 1.9 mm. The two electrode method allowed for the creation of a wide slot into which a crack mouth opening displacement transducer could be affixed, while the starter notch was finished with a thin slot to achieve the high-stress concentration effect of a small notch-root radius.

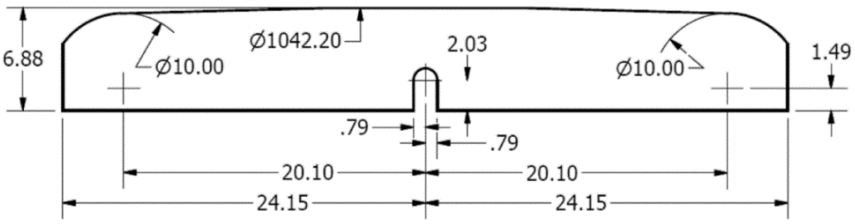

Figure 3 – EDM electrode geometry for the 1.9 mm × 48.3 mm notch geometry for the curved pipe specimens (units in mm).

2.3 Fatigue Crack Introduction

The first step in generating a reference standard for NDE evaluation of true “crack-like” features in structural materials was the development of a procedure to generate accurate and repeatable fatigue cracks in a component. The development of the fatigue-crack introduction procedure followed that outlined by Richards *et al*. [7]. The procedure depends upon the correlation between the change in a component’s stiffness and therefore compliance (the inverse of stiffness, the change in crack mouth opening displacement per unit of applied force) with a change in crack length. The compliance was measured by use of the applied force in the four-point bending arrangement by use of a load cell, and the crack mouth opening displacement (CMOD) was measured by use of an extensometer. Calibration specimens were generated by fatigue cracking notched specimens under specific conditions. During fatigue cracking, the applied loads were periodically changed to introduce characteristic fatigue striation marks on the fatigue crack surface to serve as characteristic artifacts on the fracture surface. These artifacts, termed “marker bands,” were used to correlate crack length with known compliance measurements. Upon completion of the calibration specimen run, the specimens were fractured in a brittle manner to expose the fracture surface. Figure 4 shows an example of a fatigue fracture surface with the characteristic marker bands as described below.

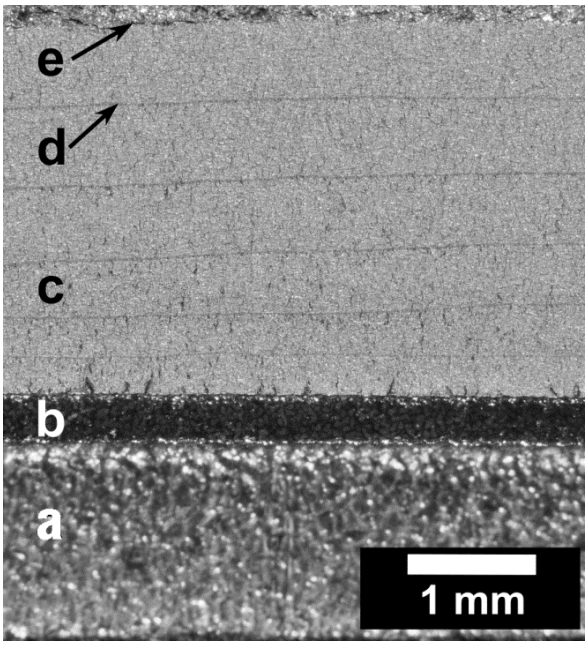

Figure 4 – Fatigue fracture surface of a fatigue crack calibration specimen. From the bottom of the image, progressively are shown (a) the surface of the thick EDM notch, (b) the thin EDM notch, (c) the fatigue crack fracture surface in which the thin, horizontal dark lines as indicated by (d) are the fatigue marker bands, and (e) finally at the top is the brittle fracture surface generated during the procedure to expose the fracture surfaces.

Closed form solutions for the stress-intensity factor, *K*, for a surface crack in a flat plate under pure bending were determined based upon ASTM E740-03, annex A2. Richards *et al*. [7] demonstrated by use of a finite element modeling that the closed form solutions for K, which are based upon linear elastic fracture mechanics (LEFM), satisfactorily predicted the stress intensity generated in a curved plate in four-point bending for the geometry shown in Figure 5. The four-point bend loading configuration for fatigue cracking of the flat plates is shown in Figure 6. The applied force levels were determined by use of a generalized relationship for steels, based upon the Paris law, in which the microstructure is composed of ferrite and pearlite as [8]:

$$\frac{da}{dN} = 6.89 \times 10^{-9} \Delta K^{3.0}, \tag{1}$$

where the fatigue crack growth rate (FCGR) *da/dN* is in units of millimeter per cycle and the stress intensity factor range ΔK is expressed in MPa$\sqrt{m}$. The ΔK levels were determined from Equation 1 in order to achieve a FCGR of approximately 0.032 µm per cycle to 0.041 µm per cycle, which results in approximately 0.5 mm of crack extension in 10,000 cycles. The selected ΔK levels were 16.7 MPa$\sqrt{m}$ for the pipe and 18.2 MPa$\sqrt{m}$ for the flat plates. The ratio of the minimum load or stress intensity factor to the maximum load or stress intensity factor, $R = 0.4$ for both the pipe and flat plate specimens.

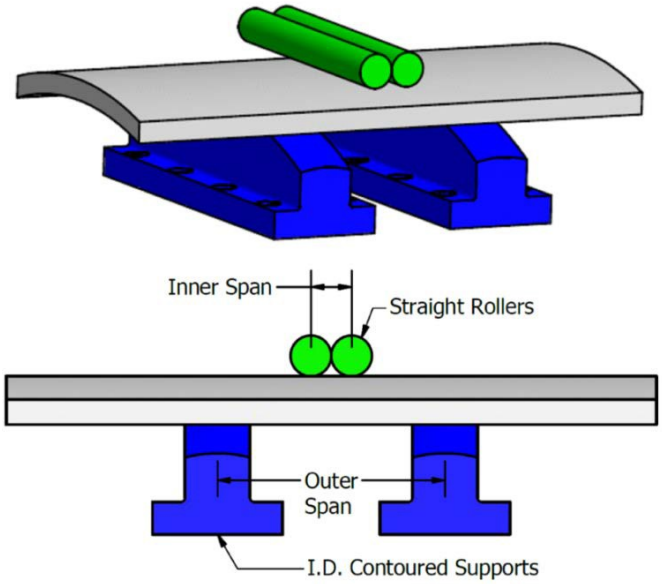

Figure 5 – Schematic of contoured loading support and straight-roller loading configuration used in four-point bending fatigue of pipe specimens.

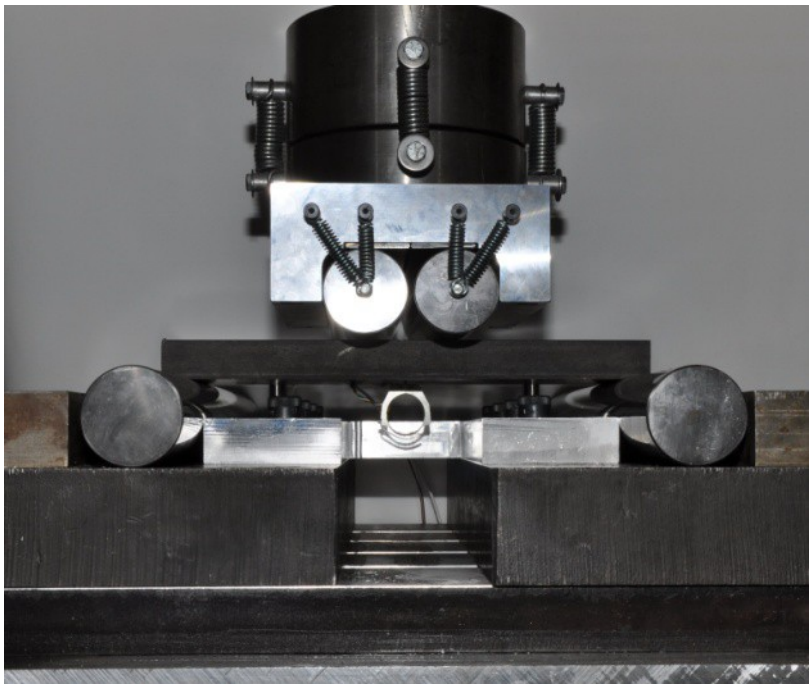

Figure 6 – Four point-bend loading configuration for fatigue crack introduction in a flat plate.

The thin, horizontal dark lines in Figure 4 are called marker bands. Marker bands are a way to introduce a characteristic feature on a fracture surface that can be used during fracture surface evaluation to identify the position of the crack front at a given point in the fatigue crack growth process. One way of producing fatigue marker bands is to change the stress intensity level during the test, which will alter the FCGR and therefore the appearance of the fatigue fracture surface generated. The fatigue marker bands were introduced through a reduction of the applied ΔK levels to 60 % of those used for the fatigue crack growth procedure listed above, i.e. $\Delta K_{\text{marker band}} = 0.6 \times \Delta K_{\text{fatigue crack growth}}$, while maintaining an $R = 0.4$, and were cyclically loaded between 50,000 cycles to 150,000 cycles per marker band. Fatigue marker bands were introduced every 10,000 cycles of fatigue crack growth at the fatigue crack growth stress intensity factor amplitude, and compliance was

measured every 1,000 cycles. Post-test, the fracture surfaces were exposed and the marker bands were measured, normal to the surface at the center of the starter notch and these data were corroborated with compliance measurements taken at the onset of the marker band introduction procedure as shown in Figure 7. Typically, three crack depth measurements were conducted for each marker band within the field of the fractograph as shown in Figure 4, and the average value was reported.

From Figure 7, the characteristic slope values relating the change in compliance with an extension of the fatigue crack are listed for the 1.067 m diameter pipe specimens having 1.9 mm x 48.3 mm notches and for the 101.6 mm and 152.2 mm wide flat plate specimens having 1.4 mm x 23.2 mm notches. The linear regression analysis of the slope of the offset compliance versus crack extension data for the 6 in wide plate data in Figure 7 was limited to a crack extension of approximately 3 mm, as the data began to deviate from linearity beyond this limit. The linear relationship between compliance change and crack extension allows for the use of a simple equation to predict the instantaneous crack length a_i in a component based upon the instantaneous compliance C_i and the initial crack length a_0 and the initial compliance, C_0 [7]:

$$a_i = \frac{C_i - C_0}{M} + a_0 \quad . \tag{2}$$

Based upon Equation 2, an initial evaluation of the ability to predict crack length from compliance data was performed. The compliance data from the calibration specimens were used to generate the compliance offset versus crack extension curves shown in Figure 7. The compliance data, in turn, were used to generate the predicted crack length versus measured crack length plot shown in Figure 8 by use of Equation 2.

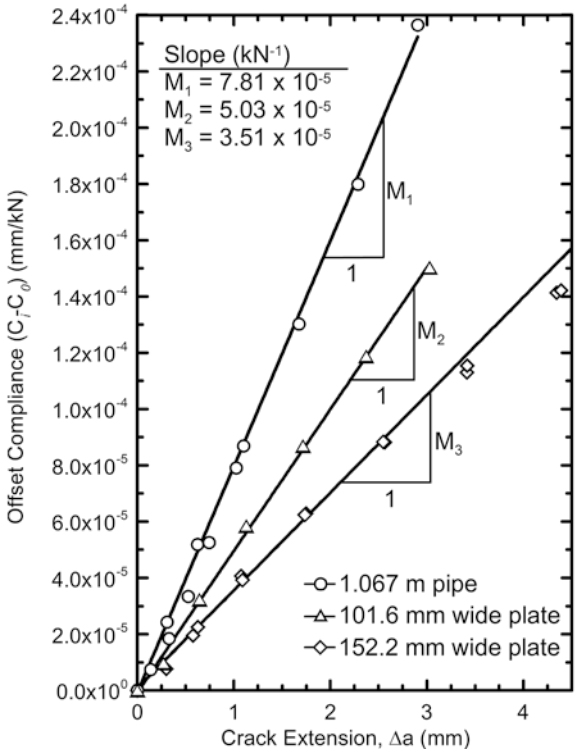

Figure 7 – Offset compliance versus crack extension measured optically from exposed fracture surfaces for the 1.067 m. diameter pipe (1.9 mm x 48.3 mm starter notch) and the 101.6 mm and 152.2 mm wide flat plates (1.4 mm x 23.2 mm starter notch).

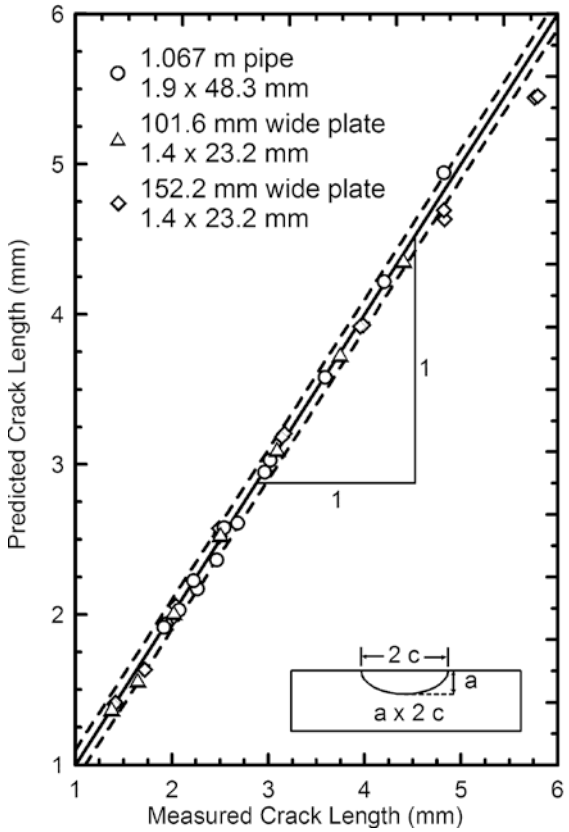

Figure 8 – Predicted versus optically measured crack length data for the 1.067 m diameter pipe (1.9 mm × 48.3 mm starter notch) and the 101.6 mm and 152.2 mm wide flat plates (1.4 mm × 23.2 mm starter notch). The dashed lines are ± 0.1 mm from the 1:1 solid line.

The data in Figure 8 demonstrate an excellent correlation between the predicted and measured crack lengths from Equation 2. The data maintain a 1:1 relationship, demonstrated by the solid line in Figure 8, and the dashed lines represent deviation limits of ± 0.1 mm from the 1:1 ratio. The data for the 1.4 mm × 23.2 mm starter notch in the 152.2 mm wide plate show a deviation from the linear response in Figure 8 at crack lengths greater than 5.5 mm, this corroborates with the deviation in the response of the compliance change with crack extensions greater than 3 mm in Figure 7.

2.3 Reference Standard Preparation

Two flat plate specimens, one 101.6 mm wide and one 152.2 mm wide, and labeled NDE SD 4-003 and NDE SD 6-002 respectively, which had EDM starter notches as shown in Figure 9, were fatigue-cracked with a target crack length of 4.4 mm. The final predicted crack length of the 102.6 mm wide plate was 4.38 mm, which was achieved at 72,000 cycles. The final predicted crack length of the 152.2 mm wide plate was 4.40 mm upon initial cracking at 61,000 cycles. However, after further evaluation of the compliance change versus crack extension data in Figure 6 for the 152.2 mm wide plates, the data at crack extensions beyond 3 mm were excluded. The result was an increase in the characteristic slope used in Equation 2. The adjusted predicted crack length for the 152.2 mm wide plate was 4.25 mm.

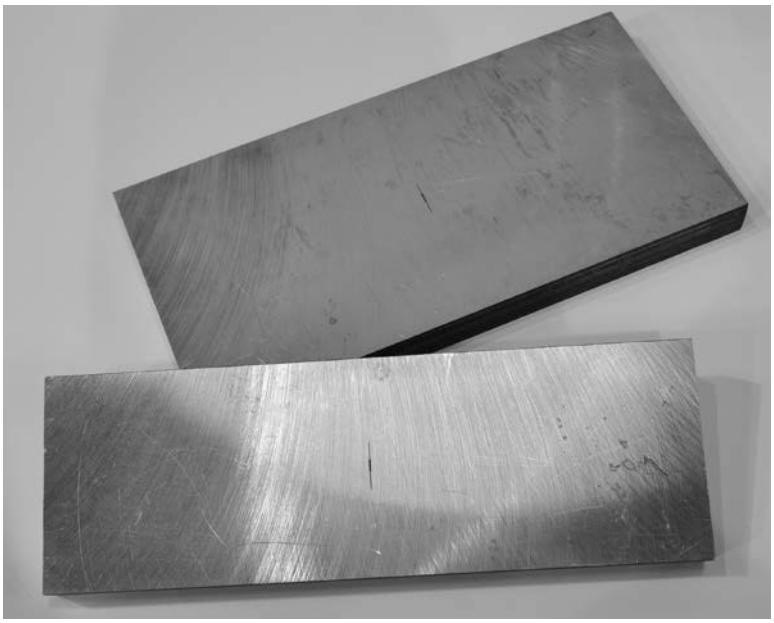

Figure 9 – Flat-plate reference standard development specimens in the EDM notched condition.

After the specimens were fatigue cracked, the thickness of the plates was reduced by Blanchard grinding, a surface machining process typically used for creating flat and parallel surfaces. The Blanchard grinding process removed the EDM starter notch through a reduction of the plate thickness. Table 1 lists the initial and final thicknesses for the 102.6 mm and 152.2 mm wide plates, along with the predicted fatigue crack length (depth from the surface) before and after Blanchard grinding.

Table 1 – Specimen thickness and predicted fatigue crack depth (*a*) values before and after Blanchard grinding

	Initial Thickness	Finish Thickness	Material Removed	Predicted Fatigue Crack Depth *a* Before Grinding	Predicted Fatigue Crack Depth *a* After Grinding
Specimen	mm	mm	mm	mm	mm
NDE SD 4-003	24.51	22.99	1.524	4.279	2.855
NDE SD 6-002	24.38	22.61	1.778	4.254	2.476

After Blanchard grinding, the specimen surface condition was such that no indication of a fatigue crack was visible. The specimens were labeled with the specimen numbers listed in Table 1, and the two faces of the specimens were labeled “A” and “B”. The specimens were wrapped in anti-corrosion paper and packaged in a hard plastic shipping crate. Along with the plates, an instruction sheet accompanied the crate to each of the collaborators providing inspection instructions. The following is the attached letter that accompanied the plates to each of the industrial collaborators.

UNITED STATES DEPA RTMENT OF COMMERCE
National Institute of Standards and Technology
325 Broadway
Boulder, Colorado 80305-3328

Thank you for participating in Phase I of the NDE reference standard development program.

The objective of Phase I is to determine the feasibility and effectiveness of using actual cracks as reference standards in the calibration of NDE sensors, methods and analysis. NIST acknowledges that flaw sizing is a complex problem with many variables for different measurement systems. The approach is to eliminate variables incrementally to obtain the highest fidelity calibration possible.

You will find two plates packaged in anti-corrosion paper. Both plates are ASTM A709 spec steel that were hot rolled to 1" thick. NDE SD-003 is nominally 4" wide and NDE SD-002 is nominally 6" wide. Both plates were ground flat and parallel. An EDM notch was put in the surface of both plates. A fatigue crack was grown in the through thickness direction and then the plates were ground again to remove the EDM starter notch.

You are invited to use any NDE method at your disposal to determine the flaw location and geometry. There are Side A and Side B reference marks and there is also an indication of which corner to use as an x-y datum for referencing the location of the flaw in each plate.

Do not use any chemicals on the plates, dye penetrant is strictly not allowed, coupling gel is permitted. Non-water-based is preferred and if surface cleaning is necessary then ethanol is acceptable. Take care to avoid exposure to water including exposure to air with more than 30% RH. Keep the plates wrapped in the anti-corrosion paper and in the shipping box when not actively being used. You are not permitted to make any permanent marks on any surface of the plate.

Make as many measurements with various sensors, methods and analysis that you feel are appropriate, these plates will be destroyed and this is your one opportunity to measure it in any way you can. NIST has provided a return shipping label to send the plates back to NIST. Along with the plates, send preliminary data on the location and geometry of the flaw. If your technique is capable of determining shape or volumetric characteristics of the flaw, please include those results as well. Your results will not be shared with other industrial collaborators and will only be used internally as a reference to determine feasibility and effectiveness of the calibration reference standards.

When Phase I is complete, the plates will be destroyed to liberate the flaw surface. At that time the surface geometry will be optically measured. NIST provide you the actual measurements when that task is complete. You are encouraged to use that data to "calibrate" your sensors, methods and analysis in anticipation of Phase II.

For technical questions or comments please contact:

Dash Weeks
303-497-5302(office)
timdash@boulcler.nist.gov

Mail Stop 853

3. Results

The plates were shipped to each industrial collaborator with an included label for shipment back to NIST, at which point the plates were shipped to the next collaborator. The collaborators were asked to provide crack geometry data such as crack depth, *a*, and width, 2*c*, when possible by use of any NDE flaw detection equipment and techniques available. Phased array ultrasonic analysis and eddy current analysis were the two methods evaluated in the present round robin study. All of the collaborators were told that the fatigue cracks were centered on the plates after that information was requested by one of the collaborators. Various sensor arrays, configurations and analysis methods were used in the Phased Array analysis. In order to retain the confidentiality of the industrial collaborators, specific details of the analysis type, sensor configuration and screenshots of the software are not presented.

3.1 Liberation of the Fatigue Crack Surface

After each of the industrial collaborators had analyzed the reference plates shown in Figure 9, the specimens were prepared for exposure of the surfaces of the fatigue crack. The sides of the specimens were saw-cut to within 25 mm of the fatigue crack edges at the surface to reduce the cross-sectional area of the specimen. The specimens were then submerged into liquid nitrogen and allowed to cool to approximately 77 K. Once thermal equilibrium was achieved, the specimens were loaded in four-point bending until catastrophic failure. The two sides of the fracture were then immersed in ethanol and allowed to warm to ambient temperature. The fractured pieces were then dried and optical fractography of the fatigue crack fracture surfaces was performed. Figure 10a shows the fatigue fracture surface of the 4 in. NDE SD specimen, and Figure 10b shows a closeup of the fatigue crack region. Figure 11a shows the fatigue fracture surface of the 6 in. NDE SD specimen, and Figure 11b shows a closeup of the fatigue crack region.

Crack depth *a* and surface breaking length 2*c* values were measured optically by use of the scale bars in Figures 10 and 11 as a reference, in which the smallest dimensional increment in the scale bar is 0.5 mm. The two sides of each broken specimen were photographed and imaged separately. The average of the two values is listed in Table 2.

Table 2 – Fatigue crack geometry estimates and optically measured values for the two reference plates.

		NDE SD 4-003	NDE SD 6-002	NDE SD 4-003	NDE SD 6-002
		Crack Depth *a*	Crack Depth *a*	Crack surface breaking length 2*c*	Crack surface breaking length 2*c*
Initial Notch Depth	mm	1.34	1.37		
Predicted Crack Depth	mm				
Prior to Notch Removal		4.379	4.254		
Final		2.855	2.476		
Measured Crack Depth	mm				
Final		3.016	2.487	18.9	17.7
Deviation from Predicted Depth (abs)		0.161	0.011		

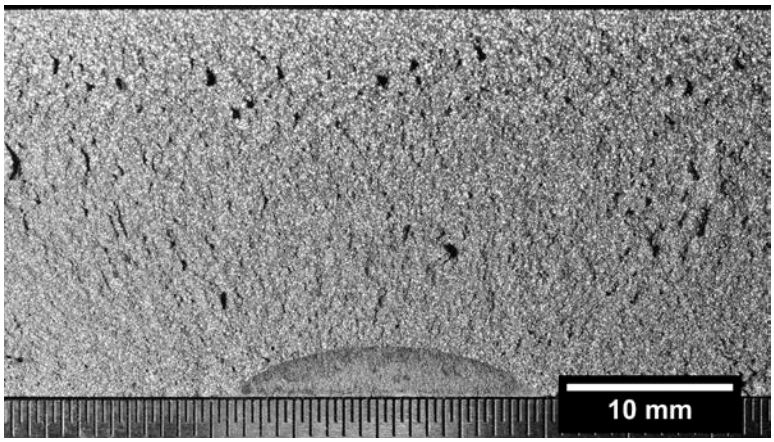

(a)

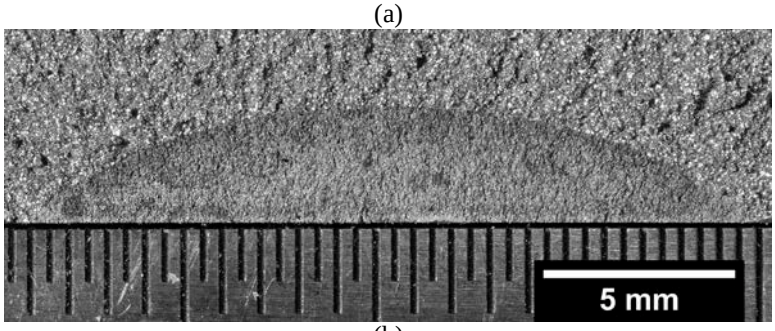

(b)

Figure 10 – Optical fractographs of exposed fatigue crack from the NDE SD 4-003 specimen, showing (a) the full specimen thickness and (b) a closeup of the fatigue crack region.

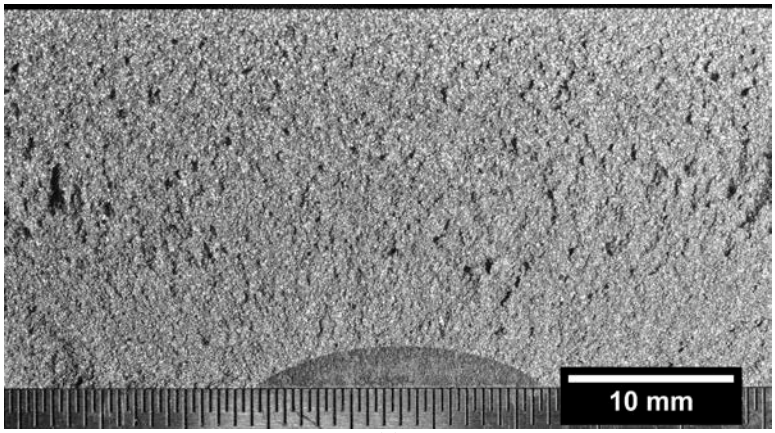

(a)

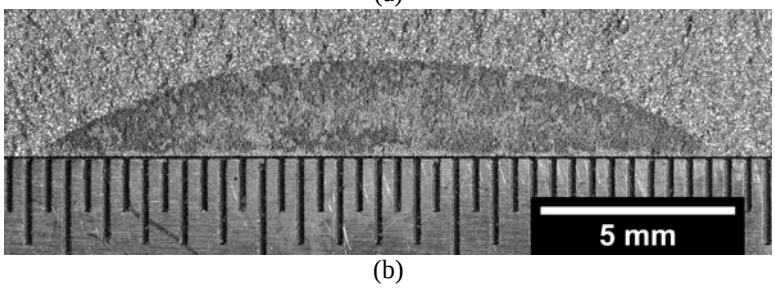

(b)

Figure 11 – Optical fractographs of exposed fatigue crack from the NDE SD 6-002 specimen, showing (a) the full specimen thickness and (b) a closeup of the fatigue crack region.

3.1 Round Robin NDE Analysis

Table 3 lists the estimated and measured crack geometry values for the two reference plates along with the reported crack depth *a*, and surface breaking length 2*c* from the industrial collaborators. The industrial collaborators are listed as #1 through #4, and the respective measurement methods are separated by numerical increments a, b, c, etc. The resolution and accuracy of the respective NDE equipment and analysis methods were not initially requested; therefore the reported values are listed with the reported number of significant figures by the respective industrial collaborator. For instances in which the values were reported in U.S. customary units (inches) the number of significant figures listed in Table 3 were selected to represent the significant figures of the reported value converted to SI units (mm). If there was no reported value for the crack depth *a* or the surface breaking length 2*c* a dash was listed for that respective position in Table 3.

Table 3 – Crack dimension values from the NDE round robin analysis for the two fatigue cracked reference plates.

			NDE SD 4-003	NDE SD 6-002	NDE SD 4-003	NDE SD 6-002
			Crack Depth *a*	Crack Depth *a*	Crack surface breaking length 2*c*	Crack surface breaking length 2*c*
Initial Notch Depth		mm	1.34	1.37		
Predicted Crack Depth		mm				
	Prior to Notch Removal		4.379	4.254		
	Final		2.855	2.476		
Measured Crack Depth		mm				
	Final		3.016	2.487	18.9	17.7
	Deviation from Predicted Depth (abs)		0.161	0.011		
Crack Length Predicted from NDE						
Collaborator						
1	Method					
	a	mm	2.44	-		
	b	mm	3.35	-		
	a	mm	3.63	1.93		
	b	mm	3.58	1.19		
2						
	a	mm	2.08	1.93	12.7	12.7
3						
	a	mm	2.1	1.9	18.5	14.5
	b	mm	-	-	11.5	17
4						
	a	mm	-	2.6	16	18
	b	mm	-	-	14	20
	c	mm	-	-	13	12
	d	mm	-	-	14	12

The omitted dimensional data in Table 3 are a result of the industrial collaborators either not being able to make the measurement due to a technical limitation of the test equipment, a technical limitation of the measurability of the reference specimen due to surface preparation or due to oversight of the collaboration statement above. Future standards development in this area will undergo different surface-preparation processes to attempt a resolution of the technical aspects of the measurability of reference specimens. Such changes include a switch from finishing the surface of the reference specimen

with Blanchard grinding processes, which are thought to impart sufficient surface deformation to "smear" the surface of the fatigue crack, to a method that has much lower surface deformation such as surface grinding. Issues associated with this change will be addressed in a future research program.

Figure 12 shows a bar chart of the deviation in crack depth measurement (a_{NDE}-$a_{Optical}$) versus the measurement number (measurement number represents each measurement method by each collaborator sequentially) for the two reference plates. Figure 12 shows that the various NDE analysis methods and collaborators both over and under-predicted the actual crack depths of the two reference plates. Figure 13 shows "bullseye" plots of the absolute value of the deviation in the values between the predicted NDE value and the optically measured value for crack depth *a* in Figure 13a and surface breaking length 2*c* in Figure 13b.

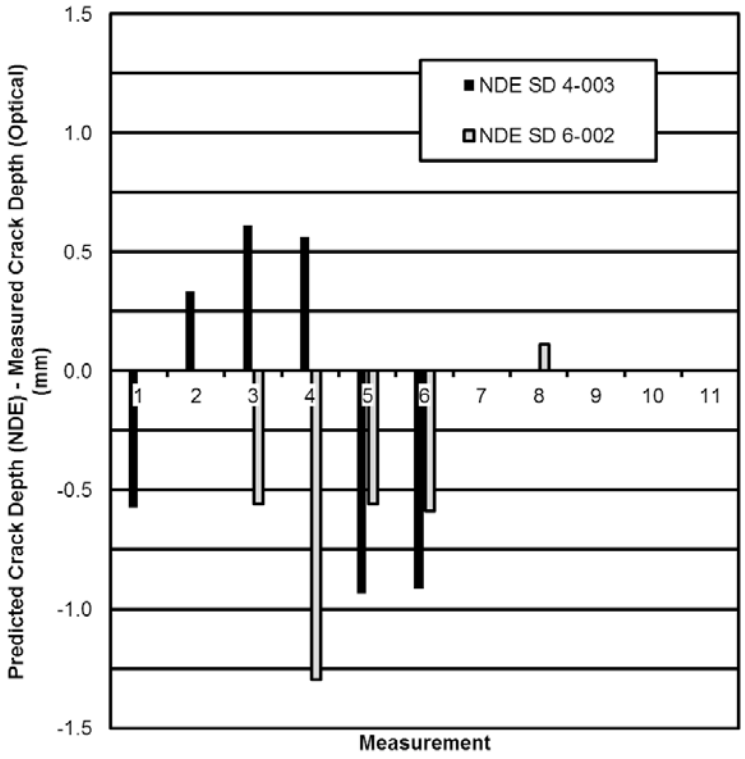

Figure 12 –Deviation of the predicted crack depth by NDE analysis to the optically measured crack depth for the two reference plates. Zero deviation indications are a result of no available data as indicated in Table 3.

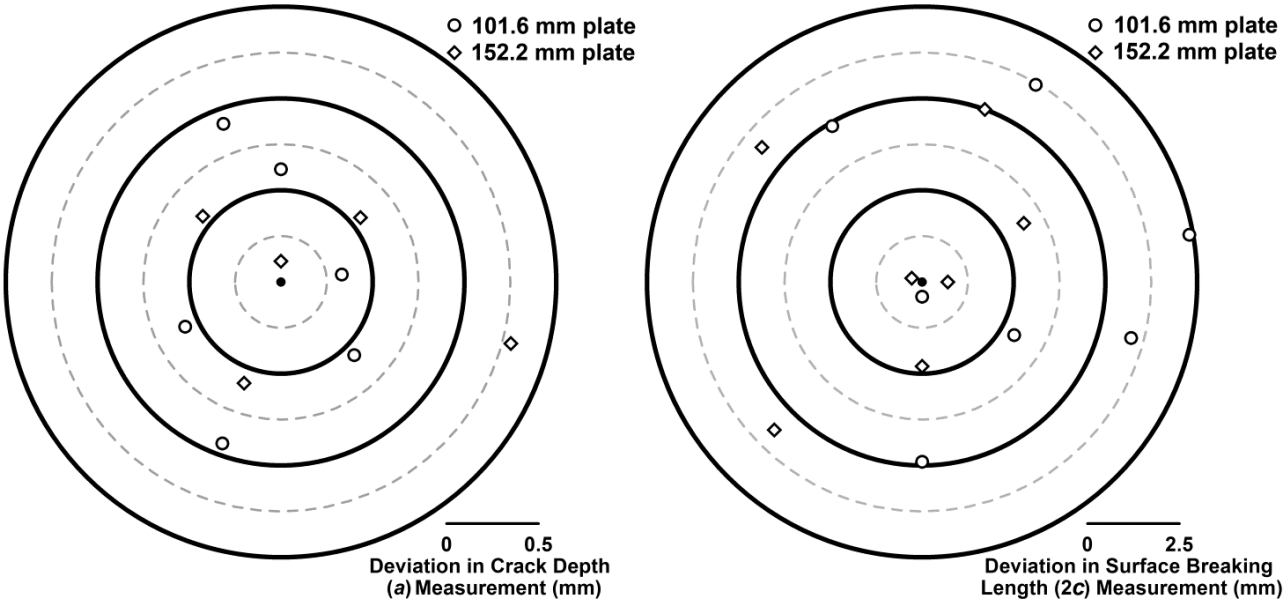

(a) (b)

Figure 13 – "Bullseye" polar plots of radius and angle, where the radius represents the deviation between the NDE predicted and actual values for crack depth *a* in Figure 13a and surface breaking crack length 2*c* in Figure 13b for the two reference plates. The angles are arbitrary. The radius scale is shown in the lower left, which represents the dimensional increment between the solid circles in each figure.

4. Discussion

In Figure 13a, the NDE analysis typically resulted in a measurement that deviated from the actual crack depth value by just over 0.5 mm, with a few measurements above this limit and a couple below. The most troubling finding here, is that for engineering critical assessment (ECA), which uses crack sizing techniques made possible by NDE technologies such as phased array ultrasonic and eddy current, the results of the round robin analysis presented here demonstrate that the NDE analysis both over-predict and under-predict the actual fatigue crack depths of the two reference plates, in some cases by substantial amounts of deviation. An over-predicted crack depth may lead to unnecessary mitigation such as repair or replacement of components, whereas an under-predicted crack depth may lead to no action, potentially leading to a catastrophic failure.

5. Conclusions

A feasibility study was successfully completed in which proposed fatigue-flaw standard-reference artifacts were developed and manufactured and were evaluated by NDE experts in collaboration with the present study. The results from the round-robin NDE analysis illustrated the need by the NDE community for such a standard, which was previously anecdotal, based upon experience with sizing real flaws by use of artificial flaws as a standard. The benefits of a representative calibration standard by which NDE sensors can be calibrated and verified should be self-evident, in that improvement of the accuracy of flaw sizing through application of verification through reference standards will decrease unnecessary costs and prevent unpredicted failure by improving structural reliability of components. The accuracy and reproducibility of the proposed fatigue crack reference standard, based upon statistical analysis, will be the focus of future work.

Acknowledgements

The Authors gratefully acknowledge the contributions of Ross Rentz and Ken Talley of NIST to this research.

Bibliography

[1] M.L. Berndt, “Non-Destructive Testing Methods for Geothermal Piping”, Report for US Department of Energy, Office of Wind and Geothermal Technologies, March 2001.

[2] S.R. Ahmed and M. Saka, “A Sensitive Ultrasonic Approach to NDE of Tightly Closed Small Cracks,” Transactions of the ASME, vol. 120, 1998, pp. 384-392.

[3] M. Yanishevsky, C. Mandache, M. Khan, A. Fahr and D. Backman, “Artificial Seeding of Fatigue Cracks in NDI Reference Coupons,” Insight, vol. 52, 2010, pp. 664-671.

[4] M. Bandyopadhyay, P.P. Nanekar, B.K. Shah, R. Ramanathan, M.D. Mangsulikar, and P.G. Kulkarni, "Ultrasonic characterization of intergranular stress corrosion cracking in austenitic stainless steel welds," Proc. 14th World Conf. on NDT, New Delhi (Dec. 1996), pp. 2197-2200.

[5] P.P. Nanekar, M. Bandyopadhyay, M.D. Mangsulikar, A.K. Bandyopadhyay, B.K. Shah and P.G. Kulkarni, "Development of in-service inspection techniques for detection of intergranular stress corrosion cracking in AISI 304 core shroud welds of boiling water reactors", Proc. Int. Conf. on Corrosion CORCON-97, Mumbai (Dec. 1997), pp. 1287-1291.

[6] L. Satyanarayan, K. Balasubramaniam, C.V. Krishnamurthy, O. Prabhakar, “Ultrasonic Phased Array for Defect Characterization,” Int. Symposium of Research Students on Material Science and Engineering, Chennai, India (Dec. 20-22, 2004).

[7] M.D. Richards, T.S. Weeks, J. D. McColskey, B. Wang, Y-Y. Wang, “Fatigue Pre-Cracking Curved Wide Plates in Bending,” Proc. 8th International Pipeline Conference, paper no. 34168,Calgary, Alberta, Canada, (September 27 – October 1, 2010).

[8] J.M. Barsom and S.T. Rolfe, *Fracture and Fatigue Control in Structures: Applications of Fracture Mechanics*, 3rd Ed., ASTM, West Conshohocken, PA, USA, 1999.